Flow, Turbulence and Combustion, September 2012, Volume 89, Issue 3, pp 385-406

External Intermittency Simulation in Turbulent Round Jets

T. Gilliland[†], K.K.J. Ranga-Dinesh[¶*], M. Fairweather[†], S.A.E.G. Falle[‡], K.W. Jenkins[¶] and A.M. Savill[¶]

[†]School of Process, Environmental and Materials Engineering, and [‡]School of Mathematics, University of Leeds, Leeds LS2 9JT, UK

[¶]School of Engineering, Cranfield University, Bedford MK43 0AL, UK

Revised Manuscript Submitted to

Flow, Turbulence and Combustion

April 2012

[*]Present Address: Engineering Department, Lancaster University, Lancaster LA1 4YR, UK

Abstract

Direct numerical and large eddy simulation (DNS and LES) are applied to study passive scalar mixing and intermittency in turbulent round jets. Both simulation techniques are applied to the case of a low Reynolds number jet with Re=2,400, whilst LES is also used to predict a high Re=68,000 flow. Comparison between time-averaged results for the scalar field of the low Re case demonstrate reasonable agreement between the DNS and LES, and with experimental data and the predictions of other authors. Scalar probability density functions (pdfs) for this jet derived from the simulations are also in reasonable accord, although the DNS results demonstrate the more rapid influence of scalar intermittency with radial distance in the jet. This is reflected in derived intermittency profiles, with LES generally giving profiles that are too broad compared to equivalent DNS results, with too low a rate of decay with radial distance. In contrast, good agreement is in general found between LES predictions and experimental data for the mixing field, scalar pdfs and external intermittency in the high Reynolds number jet. Overall, the work described indicates that improved sub-grid scale modelling for use with LES may be beneficial in improving the accuracy of external intermittency predictions by this technique over the wide range of Reynolds numbers of practical interest.

Keywords: DNS, LES, Scalar Field, Intermittency, Round Jet

1. INTRODUCTION

A round jet issuing from a circular orifice with free boundaries displays an intermittent character close to its outer edge where the flow alternates between turbulent and irrotational states. Such intermittency is frequently referred to as external intermittency to distinguish it from the internal form which concerns the variability of the energy or scalar dissipation rates [1]. External intermittency can be thought of as an indicator function that has a value of unity when the flow is turbulent and zero when it is non-turbulent, i.e. it represents the fraction of time during which a point is inside the turbulent fluid. The interface separating the turbulent and non-turbulent regions is sharp and continuously deformed by turbulent eddies of all sizes, with the interface propagating into the irrotational region while non-turbulent fluid is entrained into the turbulent flow region. The characteristics of the intermittent region are important in relation to understanding the entrainment process whereby the outer irrotational fluid becomes turbulent by acquiring vorticity. Until recently it has been assumed that this process is governed by the large-scale engulfment of irrotational fluid through the action of the dominant eddies in the turbulent flow region, although more recent investigations suggest that entrainment occurs as a results of the outward spreading of small-scale vortices [2, 4]. The intermittent behaviour of round jets is also of particular interest since it is influential in many processes of practical relevance, including mixing, combustion, emissions and aero-acoustics.

A number of experimental studies have been undertaken to investigate intermittency in various flows, including round jets, based on measurements of both the velocity and scalar fields. Townsend [5] was the first to measure intermittency in the turbulent wake generated by a circular cylinder on the basis of the flatness factor of the derivative of measured streamwise velocity fluctuations, as well as by means of an analogue technique which measured those times when fluctuating quantities could be judged non-zero. Similar approaches were subsequently used by Corrsin and Kistler [6] to measure intermittency in a round jet, a plane wake and a wall boundary layer, and by Klebanoff [7] in a boundary layer

with zero pressure gradient. Later, Becker et al. [8] used a light scattering technique to measure intermittency in a turbulent air jet, with the voltage produced by the scattered-light detection system assumed proportional to the space-averaged instantaneous concentration of a scalar in the examined spatial volume. Wygnanski and Fiedler [9] evaluated the intermittency factor in a jet on the basis of first- and second-order velocity gradients with respect to time, with Chevray and Tutu [10] employing a similar methodology to gather intermittency data in the self-preserving region of a jet that showed good agreement with the data of Corrison and Kistler [6], and Wygnanski and Fiedler [9]. Bilger et al. [11] recognised the difficulties in obtaining intermittency data when working with velocity or temperature signals, or indeed methods that used a threshold voltage, and based their measurements on probability density functions (pdfs) of a scalar in the intermittent regions of a jet flow. Nakamura et al. [12], and Schefer and Dibble [13], applied a similar approach, but adapted Bilger et al.'s [11] method of threshold evaluation in deriving intermittency values from the measured scalar pdfs.

External intermittency has also been investigated in terms of the exchange of mass, momentum and scalar quantities across the interface between the turbulent and non-turbulent regions [14, 15]. Prasad and Sreenivasan [16], and Westerweel et al. [17], used techniques based on threshold detection to identify an envelope within which the interface between the turbulent and non-turbulent flow is strongly convoluted and irrotational fluid is being engulfed. Westerweel et al. [18] outlined some characteristic features of the inhomogeneous interface between these two regions in a jet and showed the existence of a finite jump in the tangential velocity at the interface. Furthermore, these authors demonstrated that large-scale engulfment of fluid is not the dominant process for the entrainment of irrotational fluid into a turbulent jet. Theoretical analyses of intermittent flows, carried out with the aim of developing predictive procedures, have also been described by Libby [19], Dopazo [20], and Chevray and Tutu [10].

The importance of intermittency in many processes of practical relevance means that there is a clear need for the reliable prediction of turbulent intermittent flows using statistical engineering models. Direct numerical simulation (DNS) is possible, but only below the high Reynolds numbers of engineering importance, and whilst large eddy simulation (LES) can be performed at such Reynolds numbers, computer run times restrict its use in simulating many practical engineering systems. For the foreseeable future, therefore, Reynolds-averaged Navier-Stokes (RANS) techniques will remain the principal method for representing the effects of turbulence in prediction procedures for engineering application, in many industries at least.

Useful eddy viscosity-based models have been developed by Byggstoyl and Kollmann [21], and at the second-moment closure level by Janicka and Kollmann [22]. An alternative approach to modelling the influence of intermittency was suggested by Kollmann and Janicka [23] who based their predictions on pdf transport equations for a conserved scalar conditional on the fluid being turbulent, and a second scalar pdf transport equation conditional on the fluid being non-turbulent, with the rate at which non-turbulent fluid becomes turbulent being determined by an intermittency transport equation. Pope [24] also provided a similar means of accommodating intermittency effects within a joint velocity-scalar pdf framework, and more recently using a velocity-dissipation joint pdf approach [25].

Many of these methods rely on conditional averaging of the fluid flow equations, based on multiplying flow variables by an indicator function and averaging in order to incorporate the effects of intermittency. The disadvantage of this approach is that it significantly increases the number of equations needing to be solved, and presents difficulties associated with the modelling of unknown terms in the conditionally averaged equations. Cho and Chung [26] developed a technique that avoids these problems by considering the entrainment effect on intermittency in the free boundary of shear layers and deriving a set of turbulence model equations for the turbulence kinetic energy, its dissipation rate and the intermittency factor.

This approach allows the explicit incorporation of intermittency effects into the standard k-ε turbulence model, but differs from earlier closures in basing the equations on conventional Reynolds averaging rather than conditional zone averaged moments. The method therefore results in a more economical modelling approach since it decreases the number of partial differential equations that require solution. This approach was later extended to second-moment turbulence closures by Kim and Chung [27]. An alternative Reynolds stress transport-intermittency modelling approach was also successfully developed and applied to the prediction of by-pass transitional flows by Savill [28], with a similar scheme applied by Alvani and Fairweather [29] to improve predictions of scalar mixing.

However, despite the success of RANS-based approaches in modelling intermittent flows, the majority of current engineering turbulence models were derived for fully developed flows, and hence cannot be expected to provide a high degree of predictive accuracy in free shear flows where the outer regions are contaminated with irrotational flow. Also, and not withstanding intensive efforts devoted to developing more general engineering models of turbulence, their predictability is still dependent on flow configuration. The inclusion of intermittency effects within, for example, the conventional k-ε turbulence model has nevertheless been shown to resolve both the round jet/plane jet and the plane wake/plane jet anomalies [26]. Such modifications can therefore be used to increase the generality of existing turbulence models, so that further efforts directed at improving the modelling of intermittency effects are warranted, both in terms of the accuracy and generality of the models derived. This is particularly the case for the influence of intermittency on scalar fields which has received little attention.

Direct numerical and large eddy simulation are of significant benefit to the development of improved understanding of intermittency, and the derivation of more fundamentally based turbulence models, particularly in the absence of detailed experimental data on the simultaneous influence of intermittency on both the velocity and scalar fields in a jet. A

number of such studies have already been carried out for turbulent round jets. The first DNS of a spatially evolving jet was undertaken by Boersma et al. [30], with Lubbers et al. [31] extending this work to simulate the mixing of a passive scalar. Babu and Mahesh [32] also performed DNS of a round jet with upstream entrainment near the in-flow nozzle, demonstrating the importance of such entrainment on near-field behaviour, and later the same authors [33] extend their simulations to study passive scalar mixing, analysing the convective and diffusive dominated regions of the flow. Given the Reynolds number restrictions of DNS, LES has also been applied in the simulation of higher Reynolds number jets with, for example, Akselvoll and Moin [34] using LES to study turbulent confined co-annular round jets, and Mankbadi et al. [35], Boersma and Lele [36] and more recently Tucker [37] simulating the structure of compressible round jets for jet noise applications. More recently da Silva [38] carried out DNS and LES calculations for temporally evolving turbulent plane jets and analysed the behaviour of sub-grid scale models near the turbulent/non-turbulent interface. This work found that classical sub-grid scale models are unable to cope with the strong inhomogeneity of the flow near the edge of a jet. However, this work only considered conditional statistics to demonstrate the differences between the various LES sub-grid scale models employed.

To the authors' knowledge, no DNS or LES studies of round jets to date have explicitly considered external intermittency. Because of the importance of scalar mixing in a wide range of practical applications, the present work therefore studies scalar intermittency through the prediction of passive scalar pdfs using DNS and LES, and subsequently derived intermittency profiles. The study has two main aims. The first is to investigate passive scalar intermittency in a low Reynolds number round jet using both techniques with the objectives of providing improved understanding, and validating the ability of LES to predict external intermittency in a round jet flow. The second is to study scalar intermittency in a high Reynolds number round jet using the LES technique alone, again to test its ability to predict this phenomenon, this time through comparisons with experimental data. This work

is considered an essential first step in developing understanding prior to the extension of LES sub-grid scale models to explicitly consider intermittency effects, with all the simulation results at both Reynolds numbers also of value as a touchstone for the further development of RANS-based approaches for engineering application. Unlike previous investigations which considered jets both in the absence and presence of a co-flow, and in the latter case a co-flow which generally varies with radial distance (e.g. [32]), the present work uses a constant co-flow velocity for the low Reynolds number jet due to its direct relevance to engineering applications in which such boundary conditions are employed to modify jet mixing and combustion characteristics, as well as for noise reduction. The high Reynolds number jet computations also used a co-flow, in line with the experimental data used for validation purposes.

2. NUMERICAL SIMULATIONS

2.1 Governing equations and modelling

The flow is assumed to be of an incompressible and isothermal Newtonian fluid with constant properties. For DNS, the conservation equations for mass, momentum and a passive scalar, taken to be the mixture fraction, were solved as described below.

In LES the large energetic scales of motion are computed directly, with the small-scales modelled [39]. Any function is decomposed using a localised filter function, such that filtered values only retain the variability of the original function over length scales comparable to or larger than that of the filter width. In this work a top hat filter was used as this fits naturally into a finite-volume formulation. This decomposition is applied to the governing conservation equations, under the hypotheses that filtering and differentiation in space commute, giving rise to the filtered mass, momentum and passive scalar equations for the large-scale motions as follows:

$$\frac{\partial \bar{u}_j}{\partial x_j} = 0, \qquad (1)$$

$$\frac{\partial \bar{u}_i}{\partial t} + \frac{\partial \bar{u}_i \bar{u}_j}{\partial x_j} = -\frac{1}{\rho}\frac{\partial \bar{P}}{\partial x_i} - \frac{\partial}{\partial x_j}(\bar{\sigma}_{ij} + \tau_{ij}), \tag{2}$$

$$\frac{\partial \bar{\xi}}{\partial t} + \frac{\partial \bar{u}_i \bar{\xi}}{\partial x_j} = \frac{\partial}{\partial x_j}\left(\frac{\nu}{\sigma}\frac{\partial \bar{\xi}}{\partial x_j} - J_i^{sgs}\right). \tag{3}$$

Here, t is time, x_j is any of the three co-ordinate directions and u_i any of the three velocity components, p is pressure, ρ is density, ξ is the conserved scalar, ν is the kinematic viscosity, σ is the Prandtl/Schmidt number and $\bar{\sigma}_{ij} = -2\nu\bar{S}_{ij}$ is the kinematic viscous stress tensor.

The application of the filter to the non-linear convective terms in the governing equations introduces unknown terms in Eqs. (2) and (3), namely:

$$\tau_{ij} = \overline{u_i u_j} - \bar{u}_i \bar{u}_j, \tag{4}$$

$$J_j^{sgs} = \overline{u_i \xi} - \bar{u}_i \bar{\xi}. \tag{5}$$

which leaves these equations unclosed. τ_{ij} and J_j^{sgs} are, respectively, the kinematic sub-grid scale stress and the sub-grid scale scalar flux which must be modelled. The sub-grid scale stress model used was the dynamic model of Germano et al. [40], validated by that author for use in both transitional and turbulent flows, with the model implemented using the approximate localization procedure of Piomelli and Liu [41] together with the modification proposed by di Mare and Jones [42]. This model represents the sub-grid scale stress as the product of a sub-grid scale viscosity and the resolved part of the strain tensor, and is based on the possibility of allowing different values of the Smagorinsky constant at different filter levels. In this formulation the model parameter is numerically well behaved, and the method is well conditioned and avoids the irregular behaviour exhibited by some implementations of the dynamic model. Negative values of the model parameter were set to zero, with the total viscosity (molecular plus eddy) also forced to be non-negative, for reasons of numerical stability. Test-filtering was performed in all space directions, with no averaging of the

computed model parameter field, and with the filter width determined from the cube-root of the volume of a computational cell. In writing the filtered forms of the conservation equations above, it has been assumed that the filter width is invariant in space. However, this is not the case in the present work where different levels of spatial resolution are used across the solution domain, hence leading to variable grid spacing and as a result commutation error. This error can be shown to be almost entirely dissipative in nature, and estimates of this dissipation have been demonstrated to be negligible compared with dissipation of the sub-grid scale model itself. The sub-grid transport of the scalar was modelled using a gradient transport approach [43], with the sub-grid scale Prandtl/Schmidt number assigned a fixed value of 0.7 in line with recent findings [44]. Although there is uncertainty in the value of this constant, the latter value was chosen based on the results of [44], and papers cited therein, since this has been found to give good agreement with data. It also reduces computational costs relative to the use of a dynamic approach for its determination. The sensitivity of the results to the value chosen was explored, however, and found to be low.

2.2 Numerical solution

For the DNS, the conservation equations were discretised on a Cartesian mesh using a finite-volume formulation and a staggered numerical grid. Second-order central differencing was used for the spatial discretisation of all terms in both the momentum and pressure correction equations. For the passive scalar transport equation, the diffusion terms were also discretised using second-order central differencing, and to avoid the possibility of non-physical behaviour in the predicted scalar de-stablising the velocity field solution a third-order accurate and bounded scheme (SHARP - simple high-accuracy resolution program) was employed for spatial discretisation of the convection terms [45]. This scheme avoids non-physical oscillations of the scalar that can occur due to large gradients in this variable, and unphysical results such as predictions of mixture fraction outside the physically realistic range. Temporal discretisation used a second-order Crank-Nicolson scheme for the passive scalar, and a second-order hybrid Adams-Basforth/Adams-Moulton scheme for the

momentum equations. The equations, discretised as described above, were then solved using a linear equation solver. Here a bi-conjugate gradient stabilised solver with a modified strongly implicit pre-conditioner was used. The previous DNS studies by Boersma et al. [30] and Babu and Mahesh [32] used second-order central differencing for spatial discretisation, and the Adams-Bashforth scheme for time integration, similar to the methods employed in the present work.

The LES computations were performed using the computer program BOFFIN [46] which has been extensively used in the simulation of a variety of flows. The code implements an implicit finite-volume incompressible flow solver using a co-located variable storage arrangement in a Cartesian co-ordinate system. Because of the co-located arrangement, fourth-order pressure smoothing, according to the method proposed by Rhie and Chow [47], is applied to prevent spurious oscillations of the pressure field. Time advancement is performed via an implicit Gear method for all terms, with the overall procedure second-order accurate in both space and time. The time step is chosen by requiring that the maximum Courant number lies between 0.1 and 0.3, with this requirement enforced for reasons of accuracy [48]. The code is parallel and uses the message passing interface MPI-1.2. More details on the numerical algorithm and its implementation are available in [46].

2.3 Computational domain and boundary conditions

In both the DNS and LES computations of the low Reynolds number jet, fluid entered into the computational domain through a circular orifice with a top-hat velocity profile. An in-flow entrainment, in the form of a co-flow, was specified for the remaining inlet condition using a velocity of $0.1 \times U_0$, where U_0 denotes the bulk velocity at the jet inlet orifice. Free-slip boundary conditions were applied at the lateral boundaries of the computational domain and zero-normal conditions were specified at the outlet. The simulated turbulent jet had a Reynolds number, $\mathrm{Re}=U_0 D/\nu$, of 2,400, where D denotes the orifice diameter. Both

simulations were initialised using a pseudo-random velocity field with the amplitude set at 0.1% of the bulk inlet velocity U_0. It should be noted that these initial conditions are essentially identical to those employed by Babu and Mahesh [32, 33] in their DNS of a turbulent round jet in the case where the near-field region was considered to be of interest, although the present simulations used a co-flow in contrast to the buffer region employed in [32, 33] to allow upstream air entrainment. The results of the latter authors are used for comparison purposes with those of the present work below. The Reynolds number employed was chosen since it has been demonstrated [49] that the structure of low Reynolds number jets is dominated by large vortices which give rise to higher levels of flow intermittency, as compared to high Reynolds number flows.

The computational domain was represented by a cube which extended 30 jet diameters from the orifice in the cross-stream directions, and 50D downstream. The sensitivity of results to the positioning of the lateral boundaries was tested, and the predictions given below were found to be insensitive to the locations used for these boundaries. For the DNS calculations, the computational grid employed a total of 4×10^6 grid points, approximately equal to the number used by Babu and Mahesh [32], with the LES grid using a total of 1×10^6 grid points. In both cases, grid nodes were densely packed near the nozzle outlet in order to ensure adequate resolution of the circular inlet and the initial top-hat inlet profile, with the mesh expanding in both the cross-stream and streamwise directions. Tests were performed to ensure that the resolution used in the DNS calculations was sufficient to capture the local Kolmogorov microscale, and sensitivity studies performed for the LES demonstrated that the discretisation used in this case resulted in turbulence statistics that were independent of grid resolution. Tests to ensure that equivalent results were obtained at a number of angular positions were also performed. Both simulations were run over a time scale of $\approx 1200D/U_0$ to allow transients to exit the computational domain before statistics were collected. Time-averaged flow field variables reported below were computed from running averages

following this initial period, with statistics collected over approximately $900D/U_0$ to determine the mean and root mean square (rms) fluctuating values reported.

The high Reynolds number calculations carried out using LES were performed for the non-reacting propane round jet studied experimentally by Schefer and Dibble [13]. The jet nozzle had an inside diameter D = 5.26 mm and an outer diameter of 9.0 mm. The bulk average jet velocity was 53 m s^{-1} and the co-flow velocity was 9.2 m s^{-1}. Velocity measurements [13] at the jet inlet showed that the maximum velocity at the centre-line of the jet (69 m s^{-1}) was consistent with fully developed pipe flow. The Reynolds number of this jet was Re=68,000. The LES computation was performed using a non-uniform Cartesian grid in a domain with dimensions $16D \times 16D \times 75D$ in the cross-stream and streamwise directions. The computations used approximately 1×10^6 grid points, with the grids again densely packed near the nozzle outlet and expanding in both the cross-stream and streamwise directions, and with similar tests performed as for the low Reynolds number case in regards to grid resolution. Simulations were again run over a time frame that allowed initial transients to exit the computational domain before statistics were collected, with time-averaged flow field variables computed from running averages following this initial period. The boundary conditions employed were as for the low Reynolds number case, although inlet conditions for this jet were generated using a separate inflow turbulence generator based on digital filters [50]. This technique generates turbulence structures, correlated in time and space, with specified turbulence length and time scales, and was applied together with time-averaged inlet profiles obtained from experimental data [13] and RANS calculations [51].

3. RESULTS AND DISCUSSION

This section presents a detailed description of the computed scalar and external intermittency fields for the two different round jets with Re=2,400 and 68,000. The first

section describes the basis used to derive external intermittency values. The second and third sections describe DNS and LES computations of time-averaged statistics, scalar probability density function distributions and external intermittency profiles for the low and high Reynolds number round jets, respectively.

3.1 Intermittency calculations

External intermittency is essentially an indicator function which has a value of unity in the turbulent regions of a flow and zero in the non-turbulent regions. The indicator function represents the fraction of time a point is inside the turbulent fluid. Generally, a statistical tool is required for external intermittency calculations and, since intermittency is an instantaneous phenomenon, the numerical data base used for its derivation should contain only instantaneous values of corresponding variables. In the present calculations, instantaneous passive scalar values were stored at various axial and radial locations in the jets and were subsequently used to derive local probability density function distributions which were used in turn in determining the intermittency. Pdfs were determined using an approach similar to the normalised histogram method tested by Andreotti and Douady [52]. The intermittency can then be calculated using a summation of probability values above a certain threshold.

The present work adopted a similar approach to Schefer and Dibble [13] in determining intermittency values from the scalar pdfs. Probability density functions were first determined from the simulation results using, in line with Schefer and Dibble [13], no less that 8000 samples at each spatial location divided in to 50 bins equally spaced between upper and lower limits of three standard deviations from the mean, with the resulting distribution subsequently normalised so that its integral equalled unity. Given the initial distribution of $0 \le \xi \le 1$ encountered within the flows, a threshold value of $\xi_{th} = 0.015$ was then applied in deriving intermittency values. The sensitivity of intermittency values to this threshold was

examined, and in the results presented below changes in ξ_{th} of $\pm$0.005 were found to have only a small impact on the derived intermittencies.

3.2 Low Reynolds number round jet

Comparison of the predicted scalar field for the low Reynolds number round jet with Re=2,400 is made with the experimental data of Schefer and Dibble [13], Birch et al. [53], Dahm and Dimotakis [54], Dowling and Dimotakis [55], Shaughnessy and Morton [56] and Becker et al. [57], and with the DNS of Babu and Mahesh [33]. It should be noted that only the experimental data of Schefer and Dibble [13], and Shaughnessy and Morton [56], were derived in the presence of a co-flow, although the simulations of Babu and Mahesh [32] did allow some upstream air entrainment. Additionally, in comparing these results it should be borne in mind that the present predictions were derived for a low Reynolds number flow with artificially introduced turbulence, in line with case studied by Babu and Mahesh [32, 33], rather than for jets arising from fully developed turbulent pipe flow, as was generally the case for the other results considered.

Figure 1(a) shows the decay of the mean of the scalar along the jet centre-line. Both DNS and LES results show reasonable agreement, with both asymptoting to a $z\overline{\xi}_c$ value of approximately 7.0 at $z/D > 15$, which compares favourably to Schefer and Dibble [13] as the only data set to also contain the influence of a significant co-flow. Figure 1(b) shows the rms of the centre-line scalar fluctuations in terms of the unmixedness. It has been noted by Pitts [58] that there is an approximate asymptotic behaviour in this quantity that increases in value with the jet Reynolds number, and it would be anticipated that the presence of a co-flow would delay this asymptotic behaviour due to the resultant reduction in mixing. Without a co-flow, therefore, and as can be seen from the results of Babu and Mahesh [33], the unmixedness increases faster with *z*/*D* than for the present case. Dowling and Dimotakis [55] noted that whilst the mean concentration is independent of Schmidt number the scalar

fluctuations are not, with larger Schmidt numbers resulting in lower asymptotic values for the fluctuating component, as may be noted through comparison of the data of Dahm and Dimotakis [54] (Re = 5,000 and Sc = 600-800) with that of Dowling and Dimotakis [55] (Re = 5,000 and Sc = 1).

Figure 2 gives results for the radial variation of the mean scalar and the rms of its fluctuations plotted in terms of the scaled radial co-ordinate, and similarity variable, $\eta = r/(z - z_0)$. Compared to the results of other authors, reasonable agreement is found between the present predictions and those of Schefer and Dibble [13], although in general the results of Birch et al. [53], Shaughnessy and Morton [56] and Becker et al. [57] all exhibit profiles that are significantly broader in the radial direction. Differences do, however, occur due to the differing locations at which the various results were obtained, with the present simulations plotted for *z*/*D*=30, whilst those of Schefer and Dibble [13], Birch et al. [53], Shaughnessy and Morton [56] and Becker et al. [57] include data over the ranges, respectively, of $15 \le z/D \le 50$, $20 \le z/D \le 36$, $20 \le z/D \le 40$ and $20 \le z/D \le 50$.

Overall, the comparisons of Figs. 1 to 2 demonstrate reasonable agreement between the present simulations. Comparisons with the data and DNS of other authors are complicated by differences in Re, Sc and the presence or absence of any co-flow, all of which influence the development of the mixing field of a jet. The present DNS also in general shows good agreement with the data of Schefer and Dibble [13], one of only two data sets used for comparison purposes that was obtained using a co-flow.

Figures 3-6 compare derived scalar pdfs at various radial distances and at axial locations of *z/D*=10, 20, 30 and 40. Considering the centre-line evolution of the pdfs (Figs. 3-6(a)), the $P(\xi)$ distribution remains approximately Gaussian at all downstream distances, although at *z*/*D*=10 there is significant disagreement between the DNS and LES results in terms of mean

values, with significantly more mixing having taken place in the DNS, although the variance about the mean is similar in both cases. Further downstream the means come more in line, although at *z*/*D*=20 and 30 the variance in the LES results is significantly greater than in the DNS, with these differences persisting until the final downstream location. Radial variations in $P(\xi)$ can also be considered from the results of these figures. The broad, close to Gaussian distributions on the centre-line evolve with radial distance and ultimately, in terms of the DNS results shown at least, become delta functions corresponding to the ambient fluid at $\xi = 0$. Between these limits, significant skewing of the pdfs to lower values is observed, with the range of concentrations encountered at the majority of locations in general being higher for the LES-based pdfs. This also corresponds with a generally higher rate of mixing with radial distance exhibited by the DNS results at most axial locations.

Intermittency profiles derived from a large number of scalar pdfs, such as those shown in Figs. 3-6, are given in Fig. 7 for downstream axial locations of *z/D*=10, 20, 30 and 40. These results are qualitatively similar to those derived by other authors based on experimental investigations. In agreement with the scalar pdf results, in all cases the LES tends to over-estimate the width of the DNS-based intermittency profile, although reasonable agreement is obtained at *z*/*D*=10. The rate of decay of intermittency with radial distance, i.e. the rate of transition between turbulent and non-turbulent flow, is also generally under-predicted by the LES.

Since mixing is important in many applications using fully developed turbulent jets, consideration of the ability of LES to predict external intermittency values in high Reynolds number jets is necessary. The next section therefore focuses on scalar intermittency in the round jet configuration investigated experimentally by Schefer and Dibble [13]. Further discussion of the results obtained for the low Reynolds number case, particularly in the

context of the requirement for model development for LES application, is postponed until after the next section.

3.3 High Reynolds number round jet

Figure 8 (a) and (b) compares LES-based predictions of the centre-line mean scalar and the rms of its fluctuations with the experimental measurements of Schefer and Dibble [13], with good agreement found between predictions and data. Similar comparisons between LES results and data for the radial variation of the mean scalar and the rms of its fluctuations at *z/D*=15, 30 and 50 are given Fig. 9. Here, the LES results are seen to slightly over-predict the mean scalar at the centre-line, and at large radial distances at *z/D*=30 and 50, although overall good agreement is evident. In contrast, predictions of the rms scalar fluctuations are less accurate and, whilst reasonable agreement with data is obtained at *z/D*=15, significant under-prediction of the data is observed at locations further downstream close to the centre-line, with slight over-prediction at large radial distances. However, the scalar variance values are relatively small compared with the mean scalar at all axial locations, and thus some discrepancies between computational results and experimental measurements are to be expected.

Comparisons between LES results and experimental data for the scalar pdfs at various radial locations and axial distances of *z/D*=15 and 30 are shown in Figs. 10 and 11, respectively. Similar to the low Reynolds number DNS and LES pdfs, these high Reynolds number LES predictions and data show a Gaussian distribution on and close to the jet centre-line. Away from the centre-line, the pdfs again change from Gaussian and evolve with radial distance until ultimately becoming delta functions at $\xi = 0$ (although this is not seen in the pdfs of Fig. 11). Some discrepancies between predictions and data are apparent in the results of Fig. 10, particularly in terms of the mean values and the degree of skewness

in the profiles at *r/D*=0.04 and 0.32. Overall, however, the LES results are in good agreement with the experimental data at most radial locations.

Radial intermittency profiles derived from a large number of scalar pdfs, such as those shown in Figs. 10 and 11, are given in Fig. 12 for axial locations of *z/D*=15, 30 and 50. Comparison between LES-derived predictions and experimental data show good agreement, particularly in the near-field, with the gradient of the transition between turbulent and non-turbulent flow being faithfully reproduced. Some discrepancies are apparent in terms of the predictions based on the LES approach outlined in Section 2, with the predicted transition between turbulent and non-turbulent flow being displaced to larger values of *r/D* at *z/D*=30 when compared to the data, although this inconsistency is reduced by *z/D*=50 and is hardly apparent at *z/D*=15.

To confirm these findings, alternative LES predictions were derived using a totally independent approach. This separate LES solved the filtered governing equations described in Section 2 together with a sub-grid scale stress determined using the localized dynamic procedure of Piomelli and Liu [41] and the sub-grid transport of the scalar again approximated using a gradient transport approach. Solutions were obtained on a non-uniform Cartesian mesh with a staggered cell arrangement using a pressure based finite-volume method which used second-order central differencing for spatial discretisation of all terms in the momentum and pressure correction equations, and for the diffusion terms of the scalar equation. The convection term of the latter transport equation was discretised using a third-order QUICK scheme with ULTRA flux limiter [59] to ensure that the solution remained monotonic. The momentum and mixture fraction transport equations were integrated in time using a second-order hybrid Adams-Bashforth/Adams-Moulton scheme, with a Gauss-Seidel solver used to solve the system of algebraic equations resulting from the momentum and scalar equations. The BiCGStab method with a zebra Gauss-Seidel preconditioner was used to solve the algebraic equations resulting from the discretisation of pressure correction

equation. The computations used 2×10^6 grid points, twice as many the LES results considered so far. Further details on this alternative LES approach can be found in [60, 61].

The results of this study are also shown in Fig. 12 and, whilst these predictions are marginally more in line with data than those reported so far, good qualitative agreement is seen between the two LES-based results. Clearly, therefore, the sub-grid scale modelling approach employed is able to predict external intermittency to a reasonable degree of accuracy in this high Reynolds number flow, although some improvements may be necessary to completely capture the external intermittency phenomena over the whole Reynolds number range of practical interest.

3.4 Discussion

Although comparisons between time-averaged results for the scalar field of the low Reynolds number jet demonstrate reasonable agreement between the DNS and LES, significant differences do occur, particularly in terms of the scalar fluctuations. Similar comparisons to those given in Section 3.2 between the present DNS and LES, and the experimental data and simulations of other authors, were also made for the velocity field in this jet. These generally also confirmed reasonable agreement between the simulations and alternative results, of a similar level to that found for the scalar field, with the DNS in the main agreeing well with the data of Schefer and Dibble [62], again obtained in the presence of a co-flow. Some differences were, however, observed between the DNS and LES results. In particular, although the centreline mean axial velocity decay derived from the two simulations was in agreement up to a downstream distance of 10D, beyond this point they diverged, although the rate of decay was similar from z/D=25. Radial variations of the mean axial velocity were in reasonable agreement, but with differences apparent in the rate of decay of velocity close to the centreline, with similar comparisons for the three components of the turbulent fluctuating velocity and shear stress also showing acceptable agreement, but with the LES slightly over-predicting DNS results. All these differences do, however, feed through to the

derived scalar probability density functions which, although in reasonable qualitative agreement, demonstrate the more rapid influence of intermittency with radial distance in the jet for the DNS results. This in turn is reflected in derived intermittency results, with LES generally giving profiles that are broader than equivalent DNS predictions, with the rate of decay of intermittency with radial distance also generally under-predicted by the LES. In the case of the high Reynolds number jet, differences between predictions and intermittency data still persist, although these are now much less significant and decrease with increasing numerical resolution, with the location of and the rate of transition between turbulent and non-turbulent flow predicted to a reasonable degree of accuracy.

Clearly significant differences exist between the DNS and LES generated intermittency profiles in the low Reynolds number jet and, despite the relative success of LES in predicting intermittency in the high Reynolds number flow, there remains a requirement for simulation approaches capable of accurately predicting external intermittency, and its effects, over the wide range of Reynolds numbers of practical interest. This leads to the conclusion that improved sub-grid scale modelling within the LES may be beneficial, particularly given the increasing level of flow intermittency encountered with decreasing Reynolds number [49], and the practical relevance of such flows in many engineering applications.

In general, the present results indicate a number of avenues for future studies of external intermittency of relevance to improving the accuracy of prediction by LES. The recent experimental and numerical findings of Westerweel et al. [14, 18] and da Silva [38] also support the present conclusions, particularly in terms of the behaviour of the turbulent/non-turbulent interface in jets. The physical findings of Westerweel et al. [14, 17, 18] highlight the observation that the eddy viscosity has a non-zero and constant value in the irrotational outer flow region, and the combination of these previous and the present results leads to the conclusion that sub-grid scale models should be developed to cope with the strong inhomogeneity of the flow near the edge of a jet. Improvements in the modelling of the sub-

grid scale stress and scalar transport used in this work are therefore worthy of further investigation.

There are several methods by which allowance for intermittency might be introduced into such models. In particular, the simple prescription of a functional intermittency scaling of the sub-grid scale viscosity could be used, as could an intermittency transport equation for the sub-grid scale turbulence which could then be employed to appropriately scale the standard Smagorinsky eddy viscosity. Another alternative, more in line with the present approach, would be to extend the existing dynamic procedure by using local box estimation of the degree to which the resolved large eddy scales are space filling, and then using this estimate of intermittency to scale the sub-grid scale viscosity directly. Alternatively, the intermittency could be evaluated by comparing simulated estimates with expected (fully turbulent) values for appropriate representative quantities, notably the degree of helicity. On the other hand, the work carried out by Westerweel et al. [14, 17, 18] showed that turbulent entrainment appears to be caused by small-scale eddying motions at the outward propagating turbulent/non-turbulent interface, instead of more directly by large-scale engulfment. Therefore a fractal-based approach that has been previously used for small-scale internal intermittency might also be employed as a more comprehensive model to determine the interface dynamics associated with external intermittency [63]. Additionally, separate intermittency scaling allowance may also be needed for the scalar and velocity fields. This conclusion is in line with the findings of Yeung et al. [64] who, in their high resolution DNS of turbulent mixing in high Reynolds number flows, demonstrated that passive scalar mixing produces significantly higher intermittency in scalar gradient quantities than the associated gradient quantities of the velocity field at the very smallest scales, implying that the smallest scales of the passive scalar are more affected by the large-scale motions.

4. CONCLUSIONS

Direct numerical and large eddy simulation have been applied to study the scalar intermittency in a turbulent round jet with a Reynolds number of 2,400, with LES also applied to a high Re=68,000 flow. The simulation results for both low and high Reynolds number cases demonstrate the importance of external intermittency in scalar mixing.

Comparisons between time-averaged results for the scalar field of the low Reynolds number case show reasonable agreement between the DNS and LES, although comparisons with the data and predictions of other authors are complicated by differences in the initial conditions of the alternative results. Derived probability density functions are in reasonable qualitative agreement, although the DNS results demonstrate the more rapid influence of intermittency with radial distance in the jet. This is reflected in derived intermittency results, with LES generally giving profiles that are broader than equivalent DNS predictions, with the rate of decay of intermittency with radial distance also generally under-predicted by the LES. In the case of the high Reynolds number jet, differences between predictions and data still persist, although these are now much less significant, with the location of and rate of transition between turbulent and non-turbulent flow predicted to a reasonable degree of accuracy.

The results presented are significant for the modelling and simulation of intermittency. The work reported identifies that improved sub-grid scale models for application with LES are worthy of investigation in order to improve the accuracy of external intermittency predictions by this technique over the wide range of Reynolds numbers of practical interest. This is particularly the case given the increasing level of flow intermittency encountered with decreasing Reynolds number. Several methods by which allowance for intermittency might be introduced into such models are identified, ranging from the prescription of a simple functional intermittency scaling of the sub-grid scale viscosity, and the use an intermittency transport equation, through to extension of dynamic models using local box estimation of the

degree to which resolved large eddy scales are space filling, comparing simulations with expected fully turbulent values for appropriate representative quantities, through to the use of fractal-based approaches previously employed for small-scale internal intermittency prediction. Additionally, separate intermittency scaling allowance may also be needed for the scalar and velocity fields.

ACKNOWLEGEMENTS

This work was supported by the EPSRC and as such we are grateful for funding under grants EP/E03005X/1 and EP/E036945/1 on the Modelling and Simulation of Intermittent Flows. TG, MF and SAEGF would also like to express their gratitude to Prof W.P. Jones for providing the BOFFIN LES code and for many helpful discussions on its use. KKJR-D, KWJ and AMS would like to thank Dr. M.P. Kirkpatrick for providing the PUFFIN LES code.

REFERENCES

[1] Aguirre, R.C., Catrakis, H.J.: On intermittency and the physical thickness of turbulent fluid interfaces. J. Fluid Mech. 540, 39-48 (2005)

[2] Mathew, J., Basu, A.J.: Some characteristics of entrainment at a cylindrical turbulence boundary. Phys. Fluids 14, 2065-2072 (2002)

[3] Hunt, J.C.R., Sandham, N.D., Vassilicos, J.C., Launder, B.E., Monkewitz, P.A., Hewitt, G.F.: Developments in turbulence research: a review based on the 1999 Programme of the Isaac Newton Institute, Cambridge. J. Fluid Mech. 436, 353-391 (2001).

[4] Lipari, G., Stansby, P.K.: Review of experimental data on incompressible turbulent round jets. Flow Turb. Combust. 87, 79-114 (2011).

[5] Townsend, A.A.: Local isotropy in the turbulent wake of a cylinder. Austr. J. Sci. Res. 1, 161-174 (1948)

[6] Corrsin, S., Kistler, A.L.: Free-stream boundaries of turbulent flows. NACA Report No. 1244 (1955)

[7] Klebanoff, P.S.: Characteristics of turbulence in boundary layer with zero pressure gradient. NACA Report No. 1247 (1955)

[8] Becker, H.A., Hottel, H.C., Williams, G.C.: Concentration intermittency in jets. Tenth Symposium (International) on Combustion, The Combustion Institute, 1253-1263 (1965)

[9] Wygnanski, I., Fiedler, H.: Some measurements in the self-preserving jet. J. Fluid Mech. 38, 577-612 (1969)

[10] Chevray, R., Tutu, N.K.: Intermittency and preferential transport of heat in a round jet. J. Fluid Mech. 88, 133-160 (1978)

[11] Bilger, R.W., Antonia, R.A., Sreenivasa, K.R.: Determination of intermittency from the probability density function of a passive scalar. Phys. Fluids 19, 1471-1474 (1976)

[12] Nakamura, I., Sakai, Y., Tsunoda, H.: On conditional statistics of the diffusion field of matter by a point source plume in uniform mean shear flow. JSME Intl. J. 32, 180-188 (1989)

[13] Schefer, R.W., Dibble, R.W.: Mixture fraction field in a turbulent non-reacting propane jet. AIAA J. 39, 64-72 (2001)

[14] Westerweel, J., Fukushima, C., Pedersen, J.M., Hunt, J.C.R.: Momentum and scalar transport at the turbulent/non-turbulent interface of a jet. J. Fluid Mech. 631, 199-230 (2009)

[15] Mellado, J.P., Wang, L., Peters, N.: Gradient trajectory analysis of a scalar field with external intermittency. J. Fluid Mech. 626, 333-365 (2009)

[16] Prasad, R.R., Sreenivasan, K.R.: Scalar interfaces in digital images of turbulent flows. Exp. Fluids 7, 259-264 (1989)

[17] Westerweel, J., Hofmann, T., Fukushima, C., Hunt, J.C.R.: The turbulent-nonturbulent interface at the outer boundary of a self-similar turbulent jet. Exp. Fluids 33, 873-878 (2002)

[18] Westerweel, J., Fukushima, C., Pedersen, J.M., Hunt, J.C.R.: Mechanics of the turbulent-nonturbulent interface of a jet. Phys. Rev. Lett. 95, 174501 (2005)

[19] Libby, P.A.: On the prediction of intermittent turbulent flows. J. Fluid Mech. 68, 273-295 (1975)

[20] Dopazo, C.: On conditioned averages for intermittent turbulent flows. J. Fluid Mech. 81, 433-438 (1977)

[21] Byggstoyl, S., Kollmann, W.: Closure model for intermittent turbulent flows. Int. J. Heat Mass Transfer 24, 1811-1822 (1981)

[22] Janicka, J., Kollmann, W.: Reynolds stress closure model for conditional variables. In Bradbury, L.J.S., Durst, F., Launder, B.E., Schmidt, F.W., Whitelaw, J.H. (eds.) Turbulent Shear Flows 4, pp. 14.13-14.17, Springer Verlag, Berlin (1984)

[23] Kollmann, W., Janicka, J.: The probability density function of a passive scalar in turbulent shear flows. Phys. Fluids 25, 1755-1769 (1982)

[24] Pope, S.B.: Calculation of a plane turbulent jet. AAIA J. 22, 896-904 (1984)

[25] Pope, S.B.: Application of the velocity-dissipation PDF model to inhomogeneous turbulent flows. Phys. Fluids A 3, 1947-1957 (1991)

[26] Cho, R., Chung, M.K.: A k-ε-γ equation turbulence model. J. Fluid Mech. 237, 301-322 (1992)

[27] Kim, S.K., Chung, M.K.: Roles of pressure transport and intermittency for computation of turbulent free shear flows. Int. J. Heat Fluid Flow 16, 194-201 (1995)

[28] Savill, A.M.: One-point closures applied to transition. In Hallbäck, M., Henningson, D.S., Johansson, A.V., Alfredsson, P.H. (eds.) Turbulence and Transition Modelling, pp. 233-268, Kluwer Academic Publishers, Dordrecht (1996)

[29] Alvani R.F., Fairweather, M.: Prediction of the ignition characteristics of flammable jets using intermittency-based turbulence models and a prescribed pdf approach. Comput. Chem. Eng. 32, 371-381 (2008)

[30] Boersma, B.J., Brethouwer, G., Nieustadt, F.T.M.: A numerical investigation of the effect of the inflow conditions on a self-similar region of a round jet. Phys. Fluids 10, 899-909 (1998)

[31] Lubbers, C.L., Brethouwer, G., Boersma, B.J.: Simulation of the mixing of a passive scalar in a round turbulent jet, Fluid Dynam. Res. 28, 189-208 (2001)

[32] Babu, P.C., Mahesh, K.: Upstream entrainment in numerical simulations of spatially evolving round jets. Phys. Fluids 16, 3699-3705 (2004)

[33] Babu, P.C., Mahesh, K.: Direct numerical simulation of passive scalar mixing in spatially evolving turbulent round jets. AIAA Paper 2005-1121 (2005)

[34] Akselvoll, K., Moin, P.: Large-eddy simulation of turbulent confined coannular jets. J. Fluid Mech. 315, 387-411 (1996)

[35] Mankbadi, R.R., Hayder, M.E., Povinelli, L.A.: Structure of supersonic jet flow and its radiated sound. AIAA J. 32, 897-906 (1994)

[36] Boersma, B.J., Lele, S.K.: Large eddy simulation of a Mach 0.9 turbulent jet. AIAA Paper 99-1874 (1999)

[37] Tucker, P.: The LES model's role in jet noise. Prog. Aero. Sci. 44, 427-436 (2008)

[38] da Silva, C.B.: The behaviour of sub-grid models near the turbulent/nonturbulent interface in jets. Phys. Fluids 21, 081702 (2009)

[39] Smagorinsky, J.: General circulation experiments with the primitive equations. Month. Weath. Review 91, 99-164 (1963)

[40] Germano, M.: A proposal for redefinition of the turbulent stresses in the filtered Navier-Stokes equations. Phys. Fluids 29, 2323-2324 (1986)

[41] Piomelli, U., Liu, J.: Large eddy simulation of rotating channel flows using a localized dynamic model. Phys. Fluids 7, 839-848 (1995)

[42] di Mare, F., Jones, W.P.: LES of turbulent flow past a swept fence. Int. J. Heat Fluid Flow 24, 606-615 (2003)

[43] Schmidt, H., Schumann, U.: Coherent structures of the convective boundary layer derived from large-eddy simulations. J. Fluid Mech. 200, 511-562 (1989)

[44] di Mare, F., Jones, W.P., Menzies, K.R.: Large eddy simulation of a model gas turbine combustor. Combust. Flame 137, 278-294 (2004)

[45] Leonard, B.P.: Simple high-accuracy resolution program for convective modelling of discontinuities. Int. J. Numer. Meth. Fluids 8, 1291-1318 (1988)

[46] Jones, W.P.: BOFFIN: A computer program for flow and combustion in complex geometries. Dept Mech Eng, Imperial College of Science, Technology and Medicine (1991)

[47] Rhie, C.M., Chow, W.L.: Numerical study of the turbulence flow past an airfoil with trailing edge separation. AIAA J. 21, 1525-1532 (1983)

[48] Choi, H., Moin, P.: Effect of the computational time step on numerical solutions of turbulent flow. J. Comp. Phys. 113, 1-4 (1994)

[49] Suresh, P.R., Srinivasan, K., Sundararajan, T., Das, S.K.: Reynolds number dependence of plane jet development in the transitional regime. Phys. Fluids 20, 044105 (2008)

[50] Klein, M., Sadiki, A., Janicka, J.: A digital filter based generation of inflow data for spatially developing direct numerical or large eddy simulations. J. Comp. Phys. 186, 652–665 (2003)

[51] Olivieri, D.A., Fairweather, M., Falle, S.A.E.G., Prediction of external intermittency using RANS-based turbulence modelling and a transported PDF approach, Comput. Fluids 47, 75-84 (2011)

[52] Andreotti, B., Douady, S.: On probability distribution functions in turbulence. Part 1. A regularisation method to improve the estimate of a PDF from an experimental histogram, Physica D. 132, 111-132 (1999)

[53] Birch, A.D., Brown, D.R., Dodson, M.G., Thomas, J.R.: The turbulent concentration field of a methane jet. J. Fluid Mech. 88, 431-449 (1978)

[54] Dahm, W.J.A., Dimotakis, P.E.: Measurements of entrainment and mixing in turbulent jets. AIAA J. 25, 1216-1223 (1987)

[55] Dowling, D.R., Dimotakis, P.E.: Similarity of the concentration field of gas-phase turbulent jets. J. Fluid Mech. 218, 109-141 (1990)

[56] Shaughnessy, E.J., Morton, J.B.: Laser light-scattering measurements of particle concentration in a turbulent jet. J. Fluid Mech. 80, 129-148 (1977)

[57] Becker, H.A., Hottel, H.C., Williams, G.C.: The nozzle-fluid concentration field of the round, turbulent, free jet. J. Fluid Mech. 30, 285-303 (1967)

[58] Pitts, W.M.: Reynolds number effects on the mixing behaviour of axisymmetric turbulent jets. Exp. Fluids 11, 135-141 (1991)

[59] Leonard, B.P., Mokhtari, S.: Beyond first order upwind: The ULTRA SHARP alternative for non-oscillatory steady-simulation of convection. Int. J. Numer. Meth. Eng. 30, 729-766 (1990)

[60] Ranga-Dinesh, K.K.J., Savill, A.M., Jenkins, K.W., Kirkpatrick, M.P.: LES of intermittency in a turbulent round jet with different inlet conditions. Comput. Fluids 39, 1685-1695 (2010)

[61] Ranga-Dinesh, K.K.J., Jenkins, K.W., Savill, A.M., Kirkpatrick, M.P.: Swirl effects on external intermittency in turbulent jets. Int. J. Heat Fluid Flow 33, 193-206 (2012)

[62] Schefer, R.W., Dibble, R.W.: Conditional sampling of velocity in a turbulent nonpremixed propane jet. AIAA J. 25, 1318-1330 (1987)

[63] Frisch, U., Sulem, P.L., Nelkin, M.: A simple dynamical model of intermittent fully developed turbulence, J. Fluid Mech. 87, 719-736 (1978)

[64] Yeung, P.K., Donzis, D.A., Sreenivasan, K.R.: High-Reynolds-number simulation of turbulent mixing. Phys. Fluids 17, 081703 (2005)

FIGURE CAPTIONS

Fig. 1 (a) Centre-line mean scalar (multiplied by the downstream co-ordinate z) and (b) rms scalar fluctuations (▼ Birch et al. (1978), ■ Dahm and Dimotakis (1987), ▲ Dowling and Dimotakis (1990), ◄ Schefer and Dibble (2001), · · · · · · Babu and Mahesh (2005), —— present LES, – · – present DNS).

Fig. 2 Radial variation of (a) mean scalar and (b) rms scalar fluctuations (◄ Schefer and Dibble (2001), ● Birch et al. (1978), ◇ Becker et al. (1965), ◆ Shaughnessy and Morton (1977), —— present LES, – · – present DNS).

Fig. 3 Scalar pdfs at z/D=10 and (a) r/D=0.0, (b) r/D=0.5, (c) r/D=1.5 and (d) r/D=2.0 (● DNS, ○ LES).

Fig. 4 Scalar pdfs at z/D=20 and (a) r/D=0.0, (b) r/D=1.0, (c) r/D=2.0 and (d) r/D=3.5 (● DNS, ○ LES).

Fig. 5 Scalar pdfs at z/D=30 and (a) r/D=0.0, (b) r/D=1.5, (c) r/D=2.5 and (d) r/D=4.0 (● DNS, ○ LES).

Fig. 6 Scalar pdfs at z/D=40 and (a) r/D=0.0, (b) r/D=1.0, (c) r/D=3.0 and (d) r/D=4.5 (● DNS, ○ LES).

Fig. 7 Radial variation of scalar intermittency at (a) z/D=10, (b) z/D=20, (c) z/D=30 and (d) z/D=40 (● DNS, ○ LES).

Fig. 8 Centre-line variation of (a) mean scalar and (b) rms scalar fluctuations (○ Schefer and Dibble (2001), —— present LES).

Fig. 9 Radial variation of mean scalar and rms scalar fluctuations at (a, d) *z/D*=15, (b, e) *z/D*=30 and (c, f) *z/D*=50 (○ Schefer and Dibble (2001), —— present LES).

Fig. 10 Scalar pdfs at *z/D*=15 and (a) *r/D*=0.04, (b) *r/D*=0.32, (c) *r/D*=1.20 and (d) *r/D*=1.78 (○ Schefer and Dibble (2001), ■ present LES).

Fig. 11 Scalar pdfs at *z/D*=30 and (a) *r/D*=0.01, (b) *r/D*=0.52, (c) *r/D*=1.41 and (d) *r/D*=1.99 (○ Schefer and Dibble (2001), ■ present LES).

Fig. 12 Radial variation of scalar intermittency at (a) *z/D*=15, (b) *z/D*=30 and (c) *z/D*=50 (○ Schefer and Dibble (2001), ■ present LES, □ alternative LES).

FIGURES

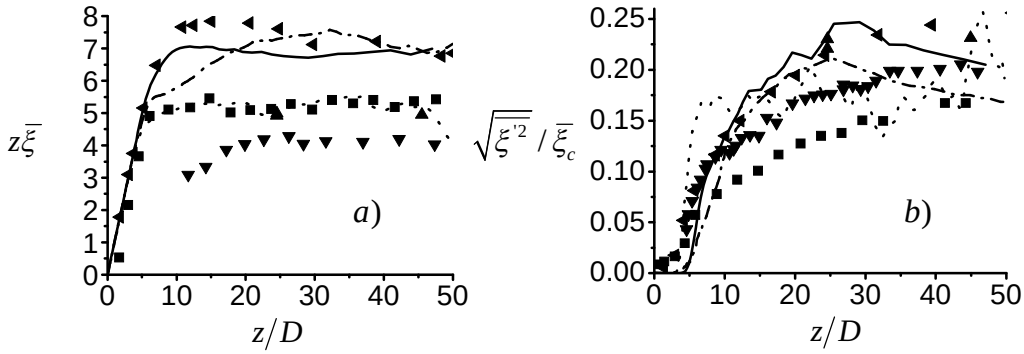

Fig. 1 (a) Centre-line mean scalar (multiplied by the downstream co-ordinate z) and (b) rms scalar fluctuations (▼ Birch et al. (1978), ■ Dahm and Dimotakis (1987), ▲ Dowling and Dimotakis (1990), ◄ Schefer and Dibble (2001), · · · · · · Babu and Mahesh (2005), —— present LES, – · – present DNS).

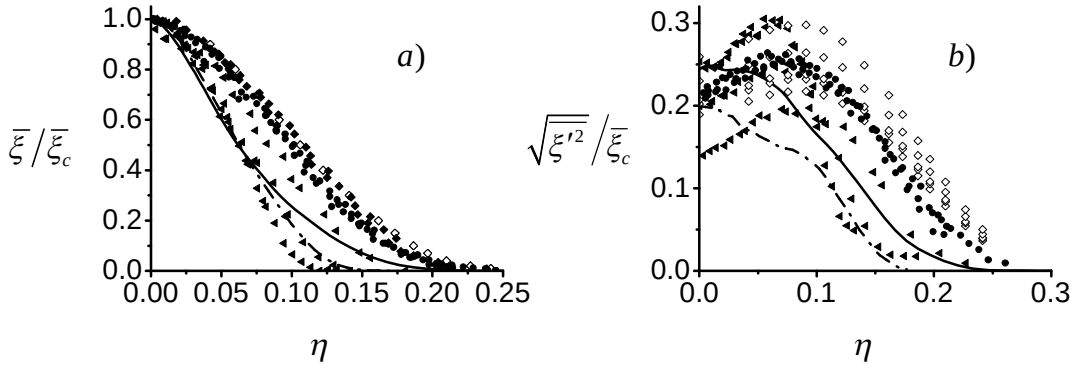

Fig. 2 Radial variation of (a) mean scalar and (b) rms scalar fluctuations (◄ Schefer and Dibble (2001), ● Birch et al. (1978), ◇ Becker et al. (1965), ◆ Shaughnessy and Morton (1977), —— present LES, – · – present DNS).

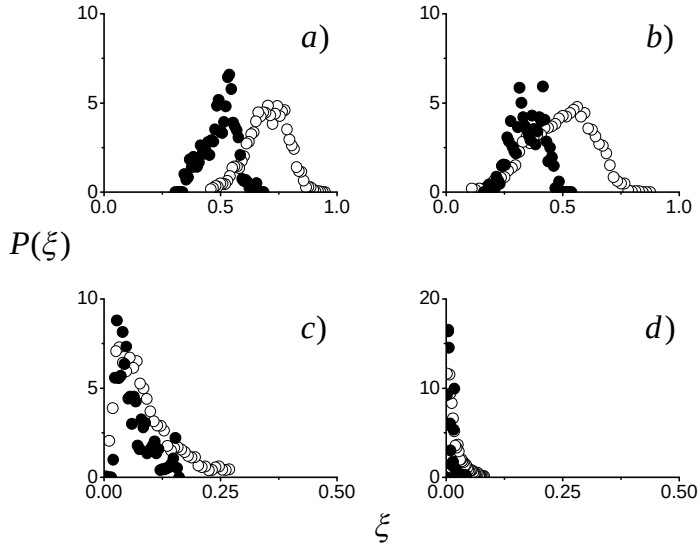

Fig. 3 Scalar pdfs at *z/D*=10 and (a) *r/D*=0.0, (b) *r/D*=0.5, (c) *r/D*=1.5 and (d) *r/D*=2.0 (● DNS, ○ LES).

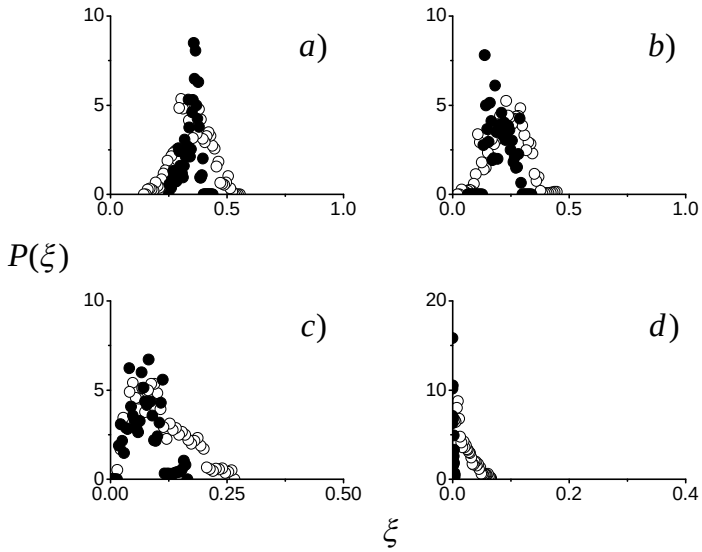

Fig. 4 Scalar pdfs at *z/D*=20 and (a) *r/D*=0.0, (b) *r/D*=1.0, (c) *r/D*=2.0 and (d) *r/D*=3.5 (● DNS, ○ LES).

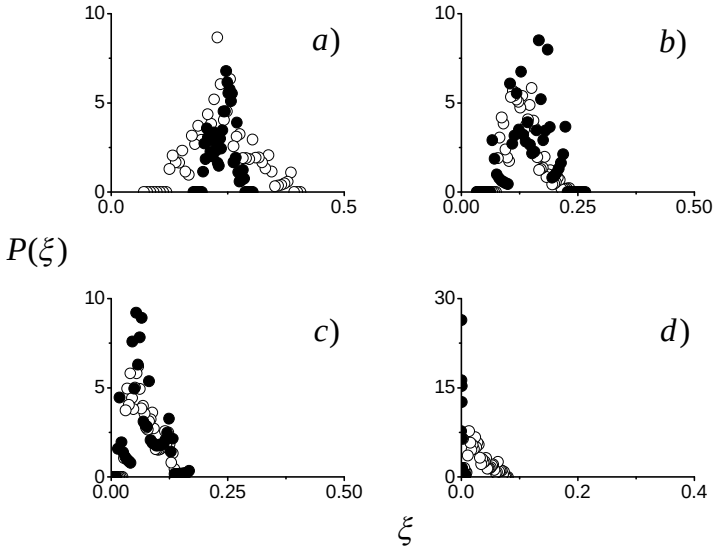

Fig. 5 Scalar pdfs at *z/D*=30 and (a) *r/D*=0.0, (b) *r/D*=1.5, (c) *r/D*=2.5 and (d) *r/D*=4.0 (● DNS, ○ LES).

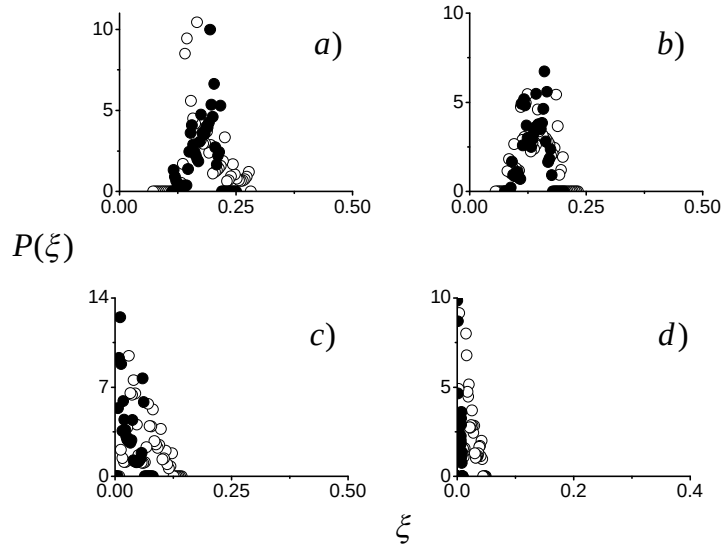

Fig. 6 Scalar pdfs at *z/D*=40 and (a) *r/D*=0.0, (b) *r/D*=1.0, (c) *r/D*=3.0 and (d) *r/D*=4.5 (● DNS, ○ LES).

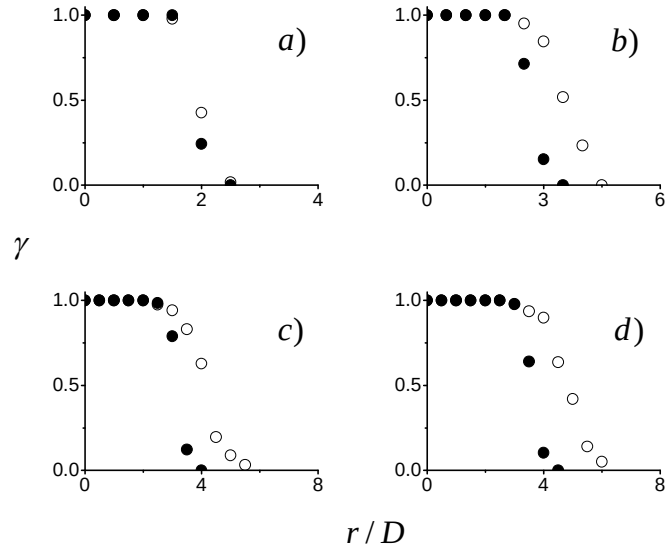

Fig. 7 Radial variation of scalar intermittency at (a) *z/D*=10, (b) *z/D*=20, (c) *z/D*=30 and (d) *z/D*=40 (● DNS, ○ LES).

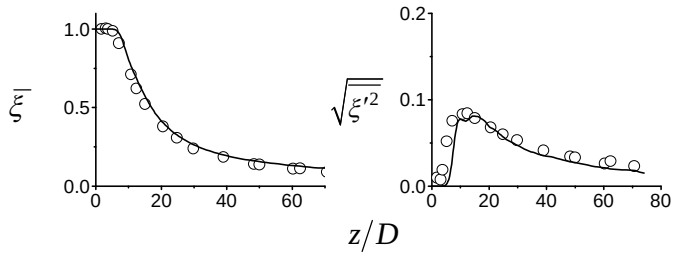

Fig. 8 Centre-line variation of (a) mean scalar and (b) rms scalar fluctuations (○ Schefer and Dibble (2001), —— present LES).

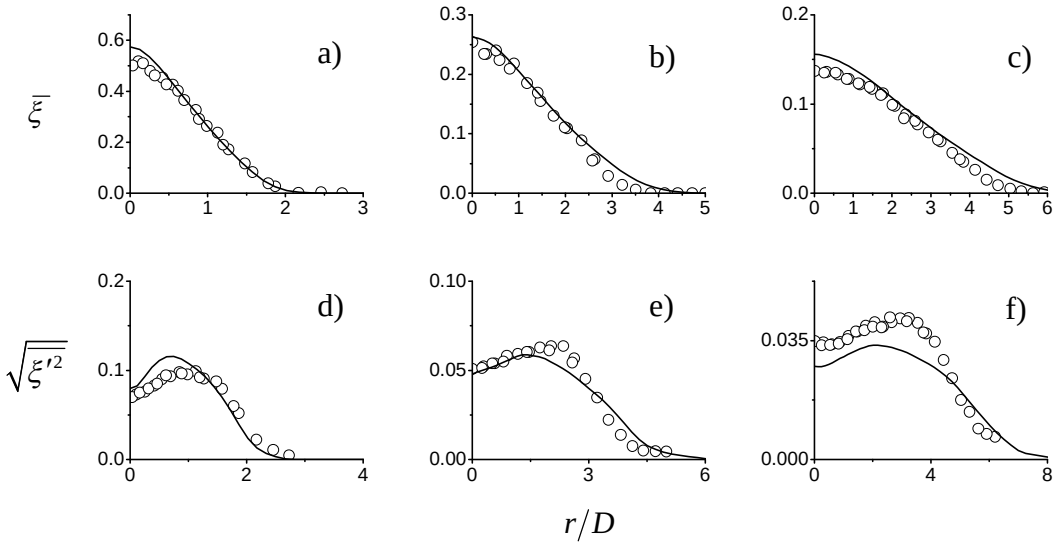

Fig. 9 Radial variation of mean scalar and rms scalar fluctuations at (a, d) *z/D*=15, (b, e) *z/D*=30 and (c, f) *z/D*=50 (○ Schefer and Dibble (2001), —— present LES).

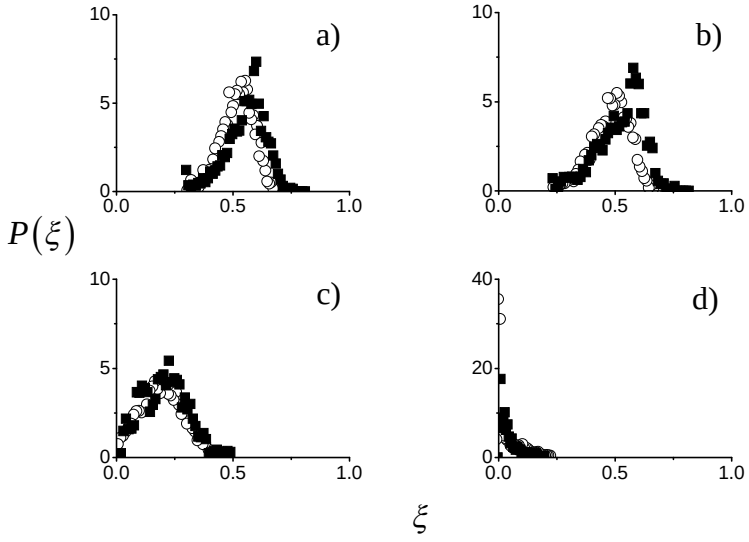

Fig. 10 Scalar pdfs at *z/D*=15 and (a) *r/D*=0.04, (b) *r/D*=0.32, (c) *r/D*=1.20 and (d) *r/D*=1.78 (○ Schefer and Dibble (2001), ■ present LES).

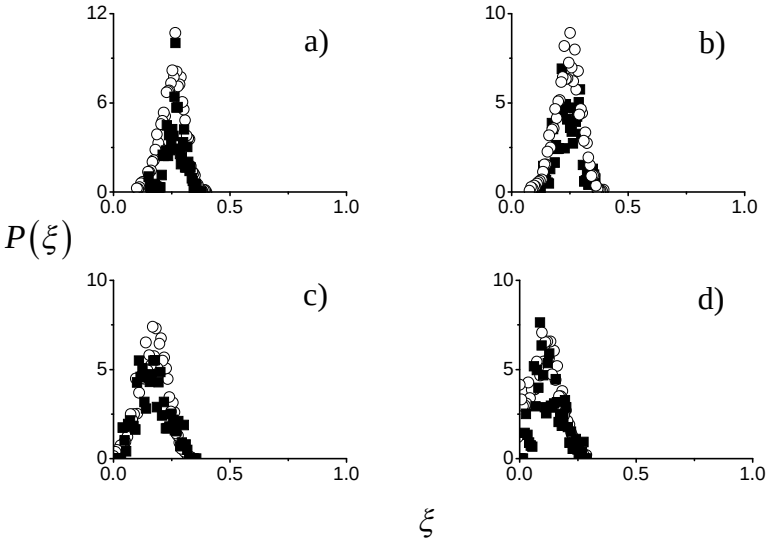

Fig. 11 Scalar pdfs at *z/D*=30 and (a) *r/D*=0.01, (b) *r/D*=0.52, (c) *r/D*=1.41 and (d) *r/D*=1.99 (○ Schefer and Dibble (2001), ■ present LES).

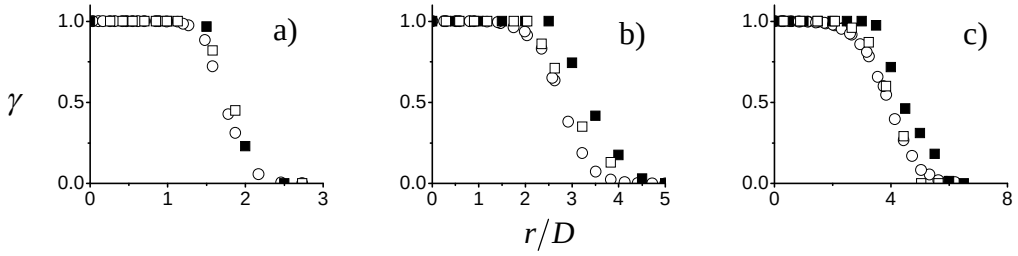

Fig. 12 Radial variation of scalar intermittency at (a) *z/D*=15, (b) *z/D*=30 and (c) *z/D*=50 (○ Schefer and Dibble (2001), ■ present LES, □ alternative LES).